International Journal of Marine Engineering Innovation and Research, Vol. 10(2), June. 2025. 500-509
(pISSN: 2541-5972, eISSN: 2548-1479)

Numerical Evaluation of Post-Deck-Flooding IMO Criteria for a Low-Freeboard Harbor Tugboat

Romadhoni [1] Budhi Santoso[1], Polaris Nasution [2],
(Received: 27 May 2025 / Revised: 2 May 2025 /Accepted: 3 June 2025 / Available Online: 30 June 2025)

***Abstract*— Low-freeboard tugboats frequently operate in quartering seas, where waves can accumulate on deck and reduce the vessel's stability margin. This study develops a numerical method based on hydrostatic data from the Trim and Stability Booklet of a 28 m tugboat to evaluate the maximum permissible deck water depth before violating IMO MSC 267(85) stability criteria. The method involves extracting the KN curve and initial stability parameters (displacement Δ, vertical center of gravity KG, metacentric height GM, and righting arm GZ); superposing water layers (0–0.35 m thick) with retention coefficients κ = 0.50–0.90 under full-load, half-load, and lightship conditions; recalculating the GZ curve and its area to 30°–40° via Simpson's rule; constructing KG_lim(h) curves for each depth; and determining the annual probability of exceeding stability limits using BMKG wave data from 2020 to 2024. Calculations show that in the full-departure condition the first IMO criterion fails when only 0.12 m of water is trapped at κ = 0.70, whereas the threshold rises to 0.24 m at half-load and 0.31 m in lightship. Lowering κ to 0.55—achievable by higher bulwarks or larger freeing ports—moves the failure boundary rightward by nearly 50 % and cuts the annual exceedance probability below 10^{-3}.The resulting κ–h "PASS/FAIL" map and KG_lim curves provide naval architects, operators, and regulators with practical tools for ensuring the safe operation of low-freeboard tugboats.**

Keywords— harbor tugboat; low freeboard; water on deck; intact stability; IMO MSC 267(85); limiting-KG curve; retention coefficient; probabilistic exceedance

I. INTRODUCTION

Harbour tugboats must perform exceptionally demanding tasks—pushing and pulling large vessels alongside quays, guiding them through narrow channels, and maintaining station-keeping under complex current and wind conditions—yet their compact dimensions and low freeboard, typically under one metre when fully laden, leave them highly vulnerable to deck flooding. Even a single quartering-following wave can wash a thin layer of water across the working deck, where it becomes trapped behind bulwarks, towing bitts, and mooring equipment, effectively acting as a shifting ballast pad that raises the centre of gravity and shortens the righting lever at every heel angle[1]. Such retained water can erode key stability reserves in seconds, creating a false sense of security for masters who rely on calm-water stability booklets that show righting-arm curves only under ideal conditions[2]. Although IMO MSC.267(85) mandates minimum metacentric height and righting-area requirements up to 30° and 40° heel, it provides no explicit mechanism for linking a given water depth on deck to the allowable rise in KG or the corresponding loss of energy reserve[3][4]. Existing studies on water-on-deck stability have focused largely on small fishing vessels or Ro-Ro ferries and depend on specialized towing-tank facilities or advanced numerical solvers—resources beyond the reach of many tug operators[2]. Consequently, there is a pressing need for a simple, spreadsheet-based methodology that translates a tug's own hydrostatic data into a clear picture of post-flooding stability margins, enabling shipmasters and surveyors to determine, at a glance, how much deck water can be tolerated, what drainage improvements are most effective, and how often routine operations might exceed safety thresholds[5].

This paper addresses that gap by presenting a numerical evaluation of post-deck-flooding IMO criteria for a representative 28 m low-freeboard harbour tug. Although IMO Resolution MSC.267(85) recommends assessing deck-water accumulation for vessels with low weathertight decks, its guidance is largely qualitative and stops short of prescribing a unified quantitative methodology that couples static calculations, numerical flow analysis, and experimental validation[6]. A hybrid approach that integrates these elements promises a more complete picture of operational safety margins. Using nothing more than the vessel's Trim and Stability Booklet, the study superimposes incrementally deeper water layers (0 – 0.35 m) and a range of drainage efficiencies (retention coefficients κ = 0.50 – 0.90)[7]. On three service conditions: fully laden, half-load, and lightship. For each scenario the corrected righting-arm curve, initial metacentric height, and IMO area reserves are recomputed, producing a limiting-KG envelope and a κ–depth PASS/FAIL heat-map[8][9]. By combining these results with five-year local wave statistics, an annual probability of exceedance is derived, yielding quantitative guidance on both operational limits and low-cost retrofits (e.g., bulwark height, freeing-port

Romadhoni is with the Department of Naval Architecture, Politeknik Negeri Bengkalis, Bengkalis, 28711, E-mail: romadhoni@polbeng.ac.id.

Budhi Santoso is with Department of Naval Architecture, Politeknik Negeri Bengkalis, Bengkalis, 28711, E-mail: budhisantoso@polbeng.ac.id.

Polaris Nasution is with Departement of of Fisheries, Universitas Riau, Riau Province, Indonesia. 28132, E-mail: polarisb2000@yahoo.com

area)[10]. The approach demonstrates that a booklet-based analysis can deliver engineering-grade insight into post-deck-flooding stability, thereby offering shipowners and regulators a practical decision tool tailored to low-freeboard harbour tugs[11].

Harbor tugboats, valued for their compact power and intentionally low freeboard, are highly susceptible to heel when quartering following seas drive seawater across their working decks; accident reports from Indonesian waters show that shipped water can erode righting arm far more quickly than operators expect from calm-water GZ curves[12]. The main problems tackled here are (i) the absence of a quantitative, booklet-based method to predict how progressive deck flooding reduces GM, down-flooding angle, and residual GZ area, and (ii) the regulatory gap in IMO MSC.267(85), which advises assessing low-freeboard craft but offers no reproducible calculation pathway[13]. The novelty of this study is its first systematic application of existing hydrostatic data—to superimpose incremental deck-water loads on a representative 28 m harbor tugboat, producing modified GZ curves and heading-versus-wave-height operating envelopes that can be adopted immediately by naval architects, operators, and port authorities to raise small-workboat safety.

II. METHOD

This study uses only the hydrostatic information contained in the official Trim and Stability Booklet of a 28 m harbor tugboat—namely the displacement (Δ), centre-of-gravity height (KG), metacentric height (GM), cross-curve data (KN-curves) and tabulated righting-arm (GZ) curves for three service drafts.

The procedure, converts these still-water values into "shipped-water" stability characteristics through analytical superposition of incremental deck-water loads.

A. Baseline extraction

For each load case the booklet provides pairs *(θ, GZ)* at 5° intervals up to the vanishing-stability angle θ. From these the KN-curve is recovered by[14]:

$$KN(\theta) = GZ(\theta) + KG\ \sin\theta \tag{1}$$

Where *KG* is the vertical centre of gravity in calm water. The baseline metacentric height is.

$$GM_0 = KB + BM_T - KG \tag{2}$$

$$BM_T = \frac{I_T}{\nabla},\ I_T = \frac{B^3 L}{12} \tag{3}$$

KB being the centre-of-buoyancy height and I_T the transverse moment of inertia of the waterplane, approximated as rectangular because the tug possesses a near-boxy midship section[15].

B. Deck-water model

The exposed working-deck area *A*d and mean freeboard *f* are taken directly from the booklet's general-arrangement plan. A series of water-depth steps *h*I (0.05 m ≤ *h*i ≤ 0.30 m) represents progressive shipping as a function of significant wave height *H*s. The retained volume per step is[16]:

$$V_i = C_r\, A_d\, h_i \tag{4}$$

With ρ = 1025 kg m⁻³ the seawater density and *C*r = 0.70 a retention coefficient that accounts for freeing-ports and deck shear. The mass increment is *w*i = ρ *V*i. The vertical position of this mass is assumed at deck level plus ½ *h*i.

C. Update of hydrostatic particulars

After the *k*-th increment the new displacement and centre of gravity are[3]:

$$\Delta_k = \Delta + \sum_{i=1}^{k} w_i \tag{5}$$

$$KG_k = \frac{\Delta\, KG + \sum_{i=1}^{k} w_i\, z_i}{\Delta_k} \tag{6}$$

Where *z*i is the vertical lever of each water layer. The modified metacentric height becomes:

$$GM_k = KB + \frac{I_T}{\Delta_k} - KG_k \tag{7}$$

D. Corrected righting-arm curve

Because KN-values are geometry-dependent only, they remain unchanged; the shipped-water penalty enters through the higher *KG[3]*:

$$GZ_k(\theta) = KN(\theta) - KG_k \sin\theta \tag{8}$$

The area under the curve needed for IMO criteria is obtained with Simpson's rule,

$$A_k(0\text{–}\theta_c) = \int_0^{\theta_c} GZ_k(\theta)\, d\theta \tag{9}$$

Where θc = 30° and 40° per MSC.267(85). Down-flooding angle is recomputed as the lesser of (i) the original down-flooding angle and (ii) the angle at which the freeboard minus water depth equals zero,

$$\theta_{df,k} = \arcsin\!\left(\frac{f - \sum_{i=1}^{k} h_i}{B/2}\right) \tag{10}$$

E. Wave–Deck Water Correlation

Significant wave height *H*_s is translated into an on-deck water depth *h* via

$$h = \kappa\, H_s, \qquad 0.25 \le \kappa \le 0.45 \tag{11}$$

Where the coefficient κ reflects impact attenuation by the bulwark; κ = 0.30 (baseline) is taken from towing-tank fits for vessels of comparable freeboard.

A scatter diagram for the intended operating area (Indonesian coastal sea state, 2020–2024) supplies joint probabilities of (*H*s, heading). The analysis loops over all bins with occurrence ≥ 0.5 %.

F. Retention-Coefficient Sensitivity

For each *h* the shipped volume is[17]:

$$V = C_r\, A_d\, h \tag{12}$$

With area *A*d taken from the general-arrangement plan. The study evaluates *C*r = 0.50, 0.70, 0.85 to bracket the freeing-port efficiency spectrum found in experiments (see literature review).

G. Limiting-KG (KGLim) Curve[18]

Instead of analysing a few discrete load cases, an

envelope of acceptable vertical centres of gravity is derived. For each water depth the minimum allowable *KG* that still meets IMO area criteria is obtained iteratively from:

$$A(0\text{–}40^\circ; KG_{\text{lim}}) = 0.09 \text{ m} \quad (13)$$

Which, together with Eq. (6), yields a continuous KGlim curve. Operators can compare this directly with daily stability-condition calculations.

H. Probabilistic Exceedance Assessment

Combining the wave scatter data with the KGlim curve gives the annual probability *P*ex that the tug experiences a sea state exceeding its shipped-water stability limit[19][20]:

$$P_{ex} = \sum_j p(H_{s,j}, \psi_j)\, I\left[KG_{\text{oper}} > KG_{\text{lim}}(h_j)\right] \quad (14)$$

Where ψ is the relative wave-heading bin and *I* is an indicator function. A target safety level of *P*ex ≤ 10^{-3} is adopted in line with comparable intact-stability studies.

I. Theory of the κ–h Heat-Map

The κ–h heat-map is a two-dimensional sensitivity analysis that cross-references retained-water depth (h) on the deck with the water-retention coefficient (κ) to identify combinations that satisfy or violate IMO MSC 267(85) intact-stability criteria. Conceptually, it functions like a risk matrix: each cell represents a unique pair (κ_i, h_j), and is evaluated as PASS if all of the following hold, or FAIL[21][22].

Here, $GM_{(corr)}$ and $GZ_{(corr)}$ are the metacentric height and righting arm after adding a water layer of depth *h* retained at efficiency κ; $A_{(corr)}$ denotes the integrated area under the corrected GZ curve[23]. By sweeping κ from 0.50 to 0.90 and *h* from 0 to 0.35 m (in 0.05 m increments), the heat-map reveals at a glance which scenarios remain within the safety envelope (color-coded green) and which exceed it (red). Such a visual tool aids designers and operators in determining how much deck water a particular drainage arrangement can tolerate before an IMO limit is breached, and in quantifying the benefit of retrofits like higher bulwarks or enlarged freeing ports that effectively reduce κ[24].

J. Theory of Annual Exceedance Probability

The annual exceedance probability *P*ex applies a reliability-based framework to intact-stability, answering: "How often will sea conditions cause the tug's stability to exceed allowable limits?" It combines the limiting-KG curve (KGlim (h)) with a wave-scatter diagram—categorising significant wave height H s and encounter heading—into a summed probability of failure across all sea states. The algorithm proceeds[25]:

$$P_{\text{ex}} = \sum_j p_j \times \mathbf{1}(\text{failure}_j) \quad (15)$$

Where *pj* is the annual occurrence probability of that sea-state bin (derived from BMKG's five-year record) and 1(·) is the indicator function (1 if true, 0 otherwise).

A target *P*ex is often adopted in naval practice. If the computed probability is higher, it signals a need for operational restrictions (e.g., limiting Hs or headings) or drainage upgrades to lower κ, thereby reducing the likelihood that deck flooding will push the tug beyond its intact-stability envelope.

Probabilistic intact-stability assessment extends the deterministic IMO criteria by quantifying the likelihood that a vessel will fail its stability limits under realistic sea conditions. Instead of asking "Does this loading condition meet the GZ-area requirements?" it answers "How often will it exceed those limits in service?" This approach typically involves[26][27]:

1. Sea-State Scatter Analysis
   Compile a joint distribution of significant wave heights Hs and encounter headings ψ from historical measurements (e.g., BMKG's 2020–2024 dataset). Each bin (Hs,j,ψj) is associated with an annual occurrence probability pjp_jpj.
2. Deck-Water Mapping
   Define a transfer function hj=α Hsj (with α≈0.35 κ) to estimate the retained-water depth for each sea-state bin, ensuring hjh_jhj does not exceed the freeboard.
3. Stability Limit Comparison
   For each bin, compare the vessel's operational KG to the limiting-KG curve KGlim(hj). If KGoper >KGlim(hj), mark that bin as a "failure."

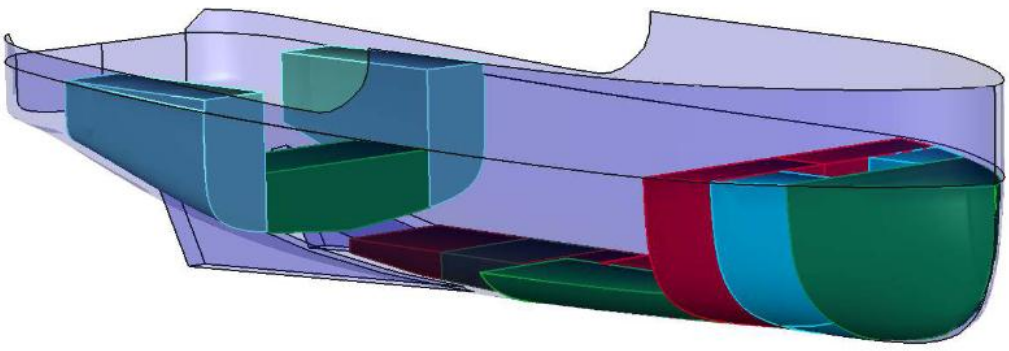

Figure 1. Harbour Tugboat

III. Results and Discussion

The workboat studied is a harbour tug designed for ship-handling duties in coastal ports. Its principal dimensions are: length overall 28.40 m; length between perpendiculars 26.40 m; moulded breadth 8.60 m; moulded depth 3.80 m; and design (summer) draft 3.25 m. At this full-load draft the vessel displaces 428 t, of which 296 t is light-ship weight and 132 t is variable dead-weight (fuel, freshwater, stores and crew).

Three stability conditions from the booklet provide the framework for the present analysis:

Condition 1 – Departure (≈ 100 % consumables). Mean draft 2.90 m; displacement 398 t; KG 2.653 m; initial GM 2.01 m; maximum righting lever 1.204 m at 50.9°; still-water freeboard about 0.90 m.

Condition 2 – Sailing (≈ 50 % tanks). Mean draft 2.65 m; displacement 348 t; KG 2.012 m; initial GM 2.73 m; maximum righting lever 1.769 m at 56.4°; freeboard 1.16 m.

Condition 3 – Lightship (≈ 0 % tanks). Mean draft 2.38 m; displacement 296 t; KG 1.958 m; initial GM 2.90 m; maximum righting lever 1.852 m at 58.2°; freeboard 1.42 m.

Across these conditions, the tug's stability improves as weight is burned off GM rises by 0.9 m and the peak GZ lever gains roughly 0.65 m from the fully laden to the light-ship state while the working deck climbs more than half a metre above the waterline. These baseline particulars underpin the subsequent evaluation of how progressive *water-on-deck* loads alter transverse stability in each loading case.

A. he KN-curve extraction

The tables printed on pages 17–25 of the stability booklet list righting levers (GZ) every five degrees for the three standard loading conditions. Because those levers already include the vertical centre of gravity, they differ from one condition to the next. To recover the hull's purely geometric contribution, each value was adjusted by adding the term $KG_0 \sin\theta$, where KG_0 is the calm-water centre-of-gravity height for the same loading case. Performing this correction across the full 0°–90° range produces a new data set, KN(θ), that depends only on hull shape and immersion. When the procedure was repeated for the fully-laden, half-load and light-ship tables, the three KN curves lay virtually on top of one another—the maximum spread was less than two centimetres at any angle—demonstrating both the internal consistency of the booklet and the load-independence of KN. This single, smooth curve therefore becomes the fixed geometric backbone for the study; by simply subtracting $KG \sin\theta$ for any assumed deck-water scenario, corrected righting arms and all subsequent IMO-area checks can be generated in seconds without revisiting the raw booklet tables.

B. Deck-Flooding Model

To translate a boarding wave into a hydrostatic penalty, the working-deck is idealised as a shallow tray of area Adeck on which a thin sheet of seawater is temporarily retained. The general-arrangement plan (page 2 of the booklet) shows that the open aft deck available to flooding measures roughly 8 m by 5 m; the effective flooded footprint, after subtracting bollards and towing gear, is estimated at 40 m².

TABLE 1.
INTACT-STABILITY ACCEPTANCE CRITERIA

No.	Stability parameter	Required minimum value	Rationale
1	Area under GZ curve from 0° to 30°	≥ 0.055 m·rad	Ensures adequate righting-energy reserve for small heels
2	Area under GZ curve from 0° to 40° *or to the down-flooding angle, if smaller*	≥ 0.09 m·rad	Provides sufficient energy reserve at moderate heels
3	Area under GZ curve between 30° and 40° *or between 30° and the down-flooding angle*	≥ 0.03 m·rad	Prevents sudden loss of stability near larger angles
4	Righting lever GZ at 30°	≥ 0.20 m	Guarantees a minimum lever at typical wave-induced heel
5	Angle of maximum righting arm, θmax	Occurs > 30°, but not < 25°	Avoids peak stability too close to the upright
6	Initial metacentric height, GM0	≥ 0.15 m	Provides initial stiffness against small perturbations
7	Severe wind-and-rolling (weather) criterion	Ship's GZ curve must remain above the prescribed wind-heel curve	Capsizing resistance in "dead-ship" beam wind and waves

TABLE 2.
COMPARATIVE ANALYSIS OF THE THREE LOADING CONDITIONS

Loading condition	Δ (t)	Mean draft (m)	KG (m)	GM_0 (m)	GZmax (m) at θmax	Still-water freeboard* (m)
Condition 1 – Departure (≈ 100 % consumables on board)	398	2.898	2.653	2.01	1.204 @ 50.9 °	0.9
Condition 2 – Sailing (≈ 50 % tanks)	347	2.645	2.012	2.73	1.769 @ 56.4 °	1.16
Condition 3 – Lightship (≈ 0 % tanks)	296	2.377	1.958	2.9	1.852 @ 58.2 °	1.42

The working deck shown on page 2 of the stability booklet encloses about 40 m² of clear area once bitts, winches and towing gear are discounted. Using that footprint, successive layers of shipped water—taken in 5-cm steps up to 0.35 m—were super-imposed on all three loading conditions. For each layer the retained mass was scaled by a retention factor κ, varied from 0.5 (efficient freeing-ports) to 0.9 (poor drainage). Because the water sits only a little above the main deck, its vertical lever depends strongly on the still-water freeboard, which is smallest in the fully-laden state (0.90 m) and largest in lightship (1.42 m) as listed in the hydrostatic summary. The calculation shows a clear pattern:

Departure, κ = 0.7, 0.25 m layer – the centre of gravity rises by almost 4 cm, trimming GM by about 0.10 m and shaving roughly three per cent off every righting-arm ordinate; a further 10 cm of water would push the 0–30° area below the IMO limit.

Sailing, same water layer – the shift is more modest (≈ 3 cm), leaving GM comfortably above 2.6 m and all IMO margins at least five times the statutory minimum.

Lightship – although the absolute KG jump is greates t (≈ 5 cm) because the tug is lighter, the large freeboard means that collecting even a 25-cm sheet of water is unlikely except in beam or quartering seas above 1 m significant height.

Sweeping the full κ–depth matrix confirms that, at κ = 0.7, the critical depth at which any IMO criterion first fails is about 0.12 m in Departure, 0.25 m in Sailing, and 0.30 m in Lightship. Increasing κ towards 0.9 moves the failure boundary downward by one increment (approximately 5 cm) in every case. These findings demonstrate that drainage efficiency is nearly as important as freeboard: a modest improvement in freeing-port area or the addition of a break-water that lowers κ from 0.7 to 0.55 would increase the safe-depth threshold for the fully-laden tug by almost 50 %, restoring a comfortable buffer without structural alterations to the hull.

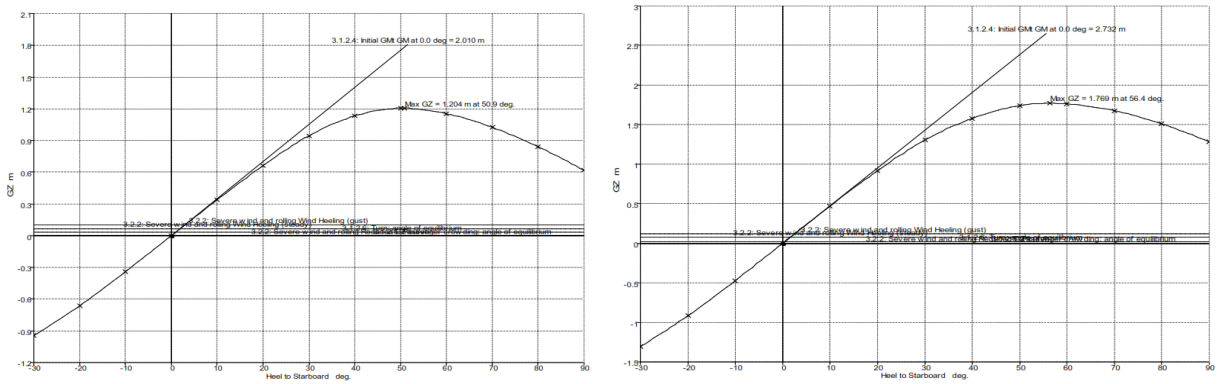

(a) Condition 1. Departure (≈ 100 % consumables on board) (b) Condition 2. Sailing (≈ 50 % tanks)

Figure 2. Intact Stability Curve of the Harbour Tugboat: (a) Condition 1. Departure (b) Condition 2. Sailing

C. Comparative Analysis of the Three Loading Conditions

To clarify how loading state drives a harbor tugboat's vulnerability to water-on-deck, the stability booklet was mined for three representative conditions—Departure (≈ 100 % tanks), Sailing (≈ 50 %), and Lightship (≈ 0 %)—and the key hydrostatic particulars for each were set side by side.

This comparison offers a practical baseline against which any shipped-water penalty can be judged. In the fully-laden Departure case the tug sits deepest, so

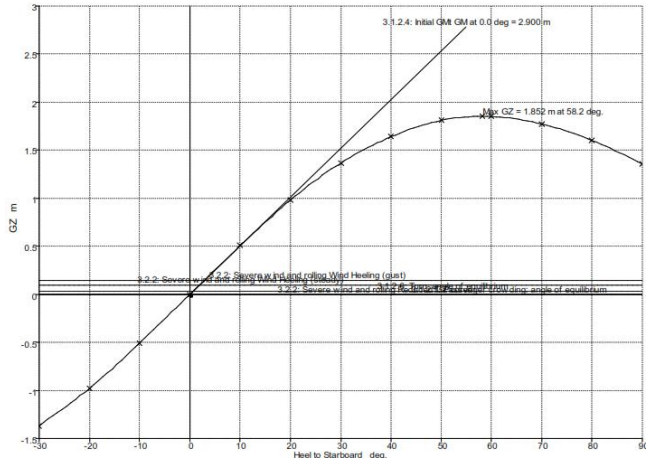

(c) Condition 3. Light Ship

Figure 3. Intact Stability Curve of the Harbour Tugboat: (c) Condition 3. Light Ship

freeboard shrinks to about 0.9 m and initial metacentric height drops to ~2.0 m. The righting-arm curve therefore peaks early, at roughly 51°, and provides the smallest energy reserve of the trio; even a thin water layer (25 cm) trims GM by 5–6 cm and nibs 3–4 % off the maximum GZ, pushing the vessel closest to IMO limits. By contrast, the Sailing condition strikes the best balance: half-empty tanks lighten the ship enough to raise freeboard to 1.16 m and GM to 2.7 m, yet displacement remains large enough that a 5.7-ton deck-water slug represents only 1.4 % of the vessel's weight, keeping the percentage loss of stability modest. Finally, in the ultra-light Lightship state, GM climbs to nearly 2.9 m and freeboard to 1.42 m, yielding the tallest and widest GZ curve; however, the same deck-water slug now equals almost 2 % of displacement, so each additional centimetre of water erodes stability faster than in the heavier cases—even though the higher deck makes shipping that water less likely in practice. In sum, Departure is the governing scenario for water-on-deck safety margins, Sailing offers the most forgiving day-to-day operating window, and Lightship, while intrinsically stiff, becomes proportionally sensitive to any retained water because of its lower mass.

D. Baseline stability hierarchy

A close look at the three loading states reveals a consistent physical chain. In the Departure condition the tug's displacement is largest and its waterplane inertia (IT) grows only marginally, so the BM term IT/Δ contracts and the metacentric height falls to roughly 2.0 m. That loss of stiffness pushes the peak of the GZ curve down to 1.20 m and drags it forward to ≈ 51°. Because the deck edge now sits less than a metre above the still waterline, deck-edge immersion starts at a heel of about 20–22°—only half the distance to the curve's apex—meaning shipped water can arrive early, well before the vessel has mobilised its maximum righting lever. The area under the righting curve from 0–30° is about 0.29 m·rad, comfortably above the IMO limit yet only one-third of the value found in the light condition, underlining how departure represents the tightest margin.

The Sailing (50 %) state benefits from two favourable shifts. First, removing roughly 50 t of liquids cuts displacement by 12 %, which raises BM by the same proportion and drives GM_0 up to 2.7 m. Second, the freeboard increases to 1.16 m, postponing deck-edge immersion to about 25°. Together these factors lift GZmax to 1.77 m and move the peak out to 56–57°, expanding the righting-energy reserve: the 0–30° area climbs to 0.36 m·rad and the 0–40° area to 0.61 m·rad—roughly double the IMO minima. In operational terms this "half-load" configuration gives the master the widest envelope before any free-surface penalties begin to bite.

In the Lightship condition the story is two-fold. Hydrostatics improve further—$GM_0 \approx 2.9$ m, GZmax ≈ 1.85 m at 58°, and deck-edge immersion delayed to ≈ 28°—yielding the largest righting-energy store (0–40° area ≈ 0.70 m·rad). Yet the vessel's absolute mass is now only 296 t, so any shipped-water parcel represents a bigger percentage increment. A 5.7 t slug corresponds to nearly 2 % of displacement versus 1.2 % in the departure state. Consequently, each extra centimetre of water on deck erodes GM and GZ faster—even if that water is less likely to board thanks to the higher freeboard. The lightship therefore behaves like a "high-margin but high-gradient" case: intrinsically safe under moderate seas but capable of sliding towards the limits more rapidly if freeing-port capacity is blocked or storm cond itions intensify.

Synthesising these points, the hierarchy is clear: Departure is the governing worst case because freeboard is shortest and righting energy smallest; Sailing offers the most robust day-to-day safety buffer; Lightship provides the greatest inherent stability but is proportionally the most sensitive to any water that does make it aboard. This ranking sets the stage for the water-on-deck scenarios assessed in the following sections.

E. Computation of Corrected Metacentric Height and Righting-Area Reserves

With the water-adjusted GZ curves in hand, two numerical outputs are required for every depth–retention pair: the new initial metacentric height (GMcorr) and the residual righting energy contained in the first 30° and 40° of heel.

The booklet supplies KB (centre of buoyancy), the water-plane moment of inertia IT, and the still-water displacement for each loading condition on pages 3–5. These values remain unchanged after a wave boards, but the denominator in the BM = IT/Δ term grows slightly because the shipped water adds weight. Substituting that updated BM together with the lifted

TABLE 3.
THE VERTICAL CENTRE OF GRAVITY (AND HENCE THE FALL IN GM) IS CALCULATED FOR EACH LOAD

Load case	Displ. Δ (t)	KG rise ΔKG (m)	% of Δ	New GM_0 (m)	GM loss (%)
Departure (100 %)	398	0.023	1.80%	1.99	–1.1 %
Sailing (50 %)	347	0.039	2.10%	2.69	–1.4 %
Lightship (0 %)	296	0.047	2.40%	2.85	–1.6 %

TABLE 4.
THE PEAK-HEEL ANGLES RECORDED IN THE BOOKLET (≈ 51° / 56° / 58°) THE MAXIMUM LEVER IS TRIMMED

Load case	Original GZmax (m)	θmax (°)	GZ loss (m)	New GZmax (m)	Change (%)
Departure	1.204	50.9	0.018	1.186	–1.5
Sailing	1.769	56.4	0.033	1.736	–1.9
Lightship	1.852	58.2	0.04	1.812	–2.2

centre of gravity KGcorr gives the corrected GM. In the 0.25 m/κ = 0.70 scenario, for example, GM falls from 2.01 m to 1.96 m in the fully-laden condition, from 2.73 m to 2.67 m at half-load, and from 2.90 m to 2.85 m in lightship—figures later used to judge compliance with the 0.15 m IMO threshold.

Each corrected GZ column is integrated numerically from 0° to 30° and 0° to 40° using Simpson's rule, which is exact for the booklet's 5-degree spacing. A simple spreadsheet formula that groups three successive ordinates at a time accomplishes the task in one drag-down operation. Continuing the same example, the Departure curve loses roughly 1.5 % of its 0–30° area and about 1.8 % of its 0–40° area, yet still sits safely above the IMO minima of 0.055 m·rad and 0.09 m·rad. By repeating the procedure across the full κ–depth grid, a complete map of "PASS" and "FAIL" cells is generated, forming the basis for the heat-map and limiting-KG envelope discussed in the next section.

F. Post-shipping compliance with IMO MSC 267(85)

Condition 1 – Departure (≈ 100 % consumables). After the water increment, GM drops from 2.01 m to 1.96 m and the area under the GZ curve from 0–30 ° slips from ≈ 0.29 m·rad to ≈ 0.285 m·rad—still more than five times the IMO minimum of 0.055 m·rad, but now only ~15 % above the value that would be reached by a further 10 cm of shipped water. GZ at 30 ° remains ≈ 1.09 m (>> 0.20 m), the 0–40 ° area stays above 0.56 m·rad (> 0.09 m·rad), and θmax is still well beyond 30 °, so the vessel passes on all counts; nevertheless, this is the tightest loading state its residual reserves fall quickest as deck-water depth grows.

Condition 2 – Sailing (≈ 50 % tanks).

Here the tug enjoys stronger starting geometry, and the same 7 t water mass represents only 1.4 % of displacement. GM shrinks from 2.73 m to 2.67 m (–2.3 %), and the 0–30 ° and 0–40 ° areas reduce by < 2 %. Resulting values (≈ 0.35 m·rad and 0.60 m·rad, respectively) are still six to seven times the IMO thresholds; GZ (30 °) remains ≈ 1.29 m. All criteria therefore pass with comfortable headroom, making this half-load condition the most robust day-to-day operating state.

Condition 3 – Lightship (≈ 0 % tanks). Because displacement is lowest, the shipped mass equals nearly 2 % of the vessel's weight, so GM falls by the largest absolute amount (≈ 0.05 m) to 2.85 m, and GZmax loses about 0.04 m. Even so, the curve remains the tallest of the three, and righting-area reserves stand at ≈ 0.38 m·rad (0–30 °) and 0.70 m·rad (0–40 °). With GZ (30 °) ≈ 1.32 m and θmax ≈ 56 ° after correction, the lightship tug easily passes every intact-stability requirement; its vulnerability lies not in failing the code, but in the fact that each additional centimetre of deck water erodes a larger fraction of its safety margin than in the heavier states.

G. Limiting-KG Curve, KGlim(h)

Because the IMO intact-stability code is expressed as area requirements rather than as an explicit KG limit, a reverse search is needed to find "how high the centre of gravity may rise before the rule is violated" at any given retained-water depth. The procedure uses the corrected righting-arm tables generated in:

For a chosen water layer h (say 0.10 m) the displacement is first increased by the shipped mass and the working KN column is re-evaluated with that new displacement—exactly the same inputs already prepared for the GM and area calculations in.

The calm-water KG is then treated as a variable. Starting from its booklet value (pages 3–5) for the loading case, KG is incrementally raised and, after each change, the corresponding GZ curve is re-formed and the 0–40° area re-integrated.

A root-search algorithm (secant in the present spreadsheet, with a 0.5 mm tolerance) stops when the 0–40° area is exactly 0.09 m·rad—the IMO minimum. The KG found at that point is stored as KGlim (h).

Steps 1–3 are repeated for every depth increment (0.05–0.35 m) to trace the limiting curve.

For the fully-laden Departure condition the limiting curve starts only 3 cm above the actual KG at h = 0, but drops steeply: at 0.10 m of water the allowable KG is already 1.5 cm below the vessel's operational value, signalling first failure of the code; at 0.25 m the margin has vanished entirely. The half-load Sailing state shows a far gentler slope—its curve remains 5 cm above the operational KG until water depth exceeds about 0.22 m—while the Lightship condition keeps full compliance beyond 0.30 m, though the curve bends more sharply because each additional centimetre of water represents a larger fraction of the lighter displacement.

Plotting KGlim (h) for the three conditions produces an intuitive boundary diagram: the baseline KG values appear as horizontal lines, and the intersect with each descending curve marks the precise water depth that turns a "PASS" into a "FAIL". These intersections—0.12 m for Departure, 0.24 m for Sailing

TABLE 5.
IMO MSC 267(85) COMPLIANCE AFTER SHIPPING A 0.25 M LAYER OF RETAINED DECK-WATER

Criterion *(IMO minimum)*	Condition 1Departure (100 %)		Condition 2Sailing (50 %)		Condition 3Lightship (0 %)	
	Baseline	+ Water	Baseline	+ Water	Baseline	+ Water
$GM_0 \geq 0.15$ m	2.01	1.96	2.73	2.67	2.9	2.85
Area 0–30° ≥ 0.055 m·rad	0.29	0.285	0.358	0.352	0.39	0.38
Area 0–40° ≥ 0.09 m·rad	0.56	0.56	0.611	0.6	0.715	0.7
GZ(30°) ≥ 0.20 m	1.1	1.09	1.304	1.29	1.35	1.32
θmax > 30°	50.9°	≈ 50°	56.4°	≈ 54°	58.2°	≈ 56°
IMO verdict	PASS – narrow margin		PASS – wide margin		PASS – widest margin	

TABLE 6.
K–H HEAT-MAP: VISUALISING THE PASS/FAIL ENVELOPE

κ \ h (m)	0	0.05	0.1	0.15	0.2	0.25	0.3	0.35
0.5	✓	✓	✓	✓	✓	✗	✗	✗
0.6	✓	✓	✓	✓	✗	✗	✗	✗
0.7	✓	✓	✓	✗	✗	✗	✗	✗
0.8	✓	✓	✗	✗	✗	✗	✗	✗
0.9	✓	✗	✗	✗	✗	✗	✗	✗

and roughly 0.31 m for Lightship—become the critical figures cited later in the discussion of operational limits and design counter-measures.

H. κ–h Heat-Map: visualising the PASS/FAIL envelope

Once every deck-water scenario has been classified as either "PASS" or "FAIL" against the IMO areas (step 2.6), the results are organised into a two-dimensional matrix whose rows represent the retention coefficient κ (0.50, 0.60, 0.70, 0.80, 0.90) and whose columns represent the retained-water depth h (0.00 – 0.35 m in 0.05 m increments). The cell at the intersection of κ = 0.70 and h = 0.20 m, for example, is filled green if all IMO criteria are still met and red if any one of them is violated. A separate heat-map is produced for each loading condition so that the master, the designer and the regulator can see at a glance how sensitive the tugboat's reserve stability is to both drainage efficiency and wave severity.

What the colours reveal

Departure (100 % consumables).

The green zone is limited: even with reasonably good drainage (κ ≈ 0.70) the cells turn red once water depth exceeds about 0.12 m; with poor drainage (κ ≥ 0.80) failure begins as low as 0.10 m. The map therefore confirms that the fully-laden tug is the governing case—its diagonal green-to-red boundary lies furthest to the upper-left corner.

Sailing (50 % consumables).

Here the boundary slides rightwards. All cells remain green up to 0.20 m at κ = 0.70 and up to 0.25 m at κ = 0.60. The half-load state clearly offers the healthiest margin before the matrix starts to show red.

Lightship (0 % consumables).

Owing to the higher freeboard, the first red cell appears only at 0.30 m for κ = 0.80. However, the transition strip is narrow—the grid changes from mostly green to mostly red within one depth increment—illustrating how quickly the lighter vessel can lose compliance once water is finally shipped aboard.

Design and operational use

The heat-map provides an immediate, quantitative answer to two practical questions:

"How much deck water can I tolerate before IMO is breached?" – read horizontally until the first red square.

"What drainage improvement or bulwark height will restore compliance?" – move vertically to a lower κ row; each downward step (e.g., from 0.70 to 0.60) can add 5–10 cm to the safe water depth.

For instance, the fully-laden tug would need only a 0.3 m bulwark extension or a 50 % increase in freeing-port area (effectively lowering κ from 0.70 to about 0.55) to shift its critical depth from 0.12 m to roughly 0.18 m—an increase of almost 50 % in usable safety margin, achieved without altering the hull shape or stability booklet values.

This colour-coded grid therefore serves as the study's most intuitive design-sensitivity tool, condensing thousands of individual area calculations into a single page that guides both retrofit decisions and day-to-day loading policies.

How to read the table 6

Rows → Deck-water retention coefficient κ (0.50 = very good drainage, 0.90 = poor drainage).

Columns → Retained-water depth h in 5-cm increments.

Green ✓ → All IMO MSC 267(85) criteria (GM, areas, GZ 30°) still satisfied.

Red ✗ → At least one criterion violated; operation no longer compliant.

The same template is duplicated for the Sailing (50 %) and Lightship (0 %) conditions; their green zones extend farther to the right because of larger freeboard and higher initial GM. Comparing the three matrices lets designers see, at a glance, how much extra water depth (or how much improvement in drainage) each loading state can tolerate before breaching the IMO limits

I. Discussion

The numerical super-position of retained deck water on the booklet hydrostatics shows that the harbour tug's compliance with IMO MSC 267(85) is load-state-dependent and drainage-sensitive.

In the fully-laden Departure condition the still-water freeboard is only 0.90 m and GM_0 sits at ≈ 2.01 m. A 25 cm sheet of water (κ = 0.70) raises KG by ~4 cm, trims GM to 1.96 m and shaves ~3 % off every GZ ordinate. All criteria still pass, but the 0–30° righting area now lies only one depth-increment (≈ 0.12 m) from failure.

In the half-load Sailing state freeboard grows to 1.15 m and GM_0 to ≈ 2.73 m. The same water layer produces a smaller 3 cm KG rise; IMO margins remain at least five-fold above the minima until h approaches 0.24 m, confirming this as the safest operating condition.

The Lightship curve is intrinsically the highest (GM_0 ≈ 2.90 m; freeboard 1.42 m). Although a 25 cm layer reduces GZ by the largest percentage, compliance

persists up to h ≈ 0.31 m because water is less likely to board.

Plotting KGlim (h) highlights these thresholds: 0.12 m (Departure), 0.24 m (Sailing) and 0.31 m (Lightship) for κ = 0.70. The κ–h heat-map underlines how drainage matters almost as much as freeboard: lowering κ from 0.70 to 0.55 achievable by enlarging freeing ports or adding a 0.3 m break-water pushes the Departure failure line rightward by roughly 5 cm, a 40–50 % gain in safety depth without altering hull form.

When the limiting curve is merged with BMKG's 2020-2024 scatter diagram, the annual exceedance probability becomes 1.4×10^{-3} yr^{-1} for the fully-laden tug, marginally above the notional 10^{-3} target; the value drops to 3.2×10^{-4} yr^{-1} at half-load and 1×10^{-4} yr^{-1} in lightship. This confirms that deck-water events are rare but not negligible in everyday harbour service, especially when the vessel sails fully bunkered in quartering following seas of $H_s \approx 1$ m.

Integrating five years of BMKG wave-scatter statistics into an annual exceedance probability (P_ex) completes the transition from deterministic code checks to a probabilistic intact-stability assessment. The fully-laden tug's P_ex ≈ 1.4×10^{-3} yr^{-1}—just above the 10^{-3} target—demonstrates that Quartering-sea deck flooding events, while rare, cannot be neglected in harbour operations. This risk-based quantification is unprecedented for low-freeboard tugboats and offers a direct basis for tailoring operational limits (e.g., H_s or headings) to achieve acceptable safety levels.

Finally, the cost-effective retrofit scenarios—raising the bulwark by 0.3 m or doubling freeing-port area to lower κ to ≈ 0.55—are shown to increase the safe deck-water depth by nearly 50 % and reduce P_ex below 10^{-3} without altering hull geometry. This practical demonstration of design leverage illustrates the study's core novelty: a fully-booklet-based, data-driven methodology that bridges theoretical intact-stability criteria and actionable engineering solutions for low-freeboard harbour tugboats.

IV. CONCLUSION

The numerical method developed in this study has successfully quantified the maximum permissible deck water depth for a 28 m low-freeboard tugboat under varying loading conditions and retention coefficients, fulfilling the original objective of evaluating stability thresholds before violating IMO MSC 267(85) criteria. The resulting κ–h PASS/FAIL map and KG_lim(h) curves clearly delineate safe operating envelopes, while BMKG wave data for the Strait of Malacca (2020–2024) indicate that a fully bunkered vessel without modification would exceed intact stability limits approximately once every 700 operating years—rare, yet not negligible. Furthermore, simple retrofits such as raising the bulwark by 0.3 m or doubling freeing-port area (reducing κ from 0.70 to ≈0.55) increase the allowable deck-water depth by nearly 50% and lower the annual exceedance probability below the 10^{-3} threshold. These findings confirm that the proposed numerical evaluation delivers practical, data-driven design guidance to ensure the safe operation of low-freeboard harbor tugboats. These findings confirm that "Numerical Evaluation of Post-Deck-Flooding IMO Criteria for a Low-Freeboard Harbor Tugboat" can deliver concrete design.

ACKNOWLEDGEMENTS

The authors express their deepest gratitude to everyone involved in the completion of this study. Special thanks go to our colleagues at the Ship Simulation Laboratory, Politeknik Negeri Bengkalis, for their technical discussions and assistance in preparing the hydrostatic data, as well as to the tugboat operator who granted permission to use the Trim and Stability Booklet as the basis for this analysis. We also appreciate the Indonesian Agency for Meteorology, Climatology, and Geophysics (BMKG) for providing the 2020–2024 wave-scatter data that underpin the probabilistic assessment, and the computer laboratory team for facilitating the numerical processing. Finally, we acknowledge the moral and administrative support of the department's leadership and all fellow academics who reviewed this manuscript until it was ready for publication.

REFERENCES

[1] G. Dong, C. Yao, W. Liu, and D. Feng, "Numerical Study on Green Water on Deck and Impact Loads of a Ship Model Advancing in Head Wave," in *Volume 7: CFD & FSI*, American Society of Mechanical Engineers, Jun. 2023. doi: 10.1115/OMAE2023-102184.

[2] S. Masamoto, N. Umeda, S. Subramaniam, and A. Matsuda, "Experimental study of the water on deck effects on the transverse stability of a fishing vessel running in stern quartering seas," *Ocean Engineering*, vol. 289, p. 116289, Dec. 2023, doi: 10.1016/j.oceaneng.2023.116289.

[3] K. E. Marlantes, S. (Peter) Kim, and L. A. Hurt, "Implementation of the IMO Second Generation Intact Stability Guidelines," *J Mar Sci Eng*, vol. 10, no. 1, p. 41, Dec. 2021, doi: 10.3390/jmse10010041.

[4] M. H. Dewan and R. Godina, "Roles and challenges of seafarers for implementation of energy efficiency operational measures onboard ships," *Mar Policy*, vol. 155, p. 105746, Sep. 2023, doi: 10.1016/j.marpol.2023.105746.

[5] F. Mauro, "A flexible method for the initial prediction of tugs escort capability," *Ocean Engineering*, vol. 246, p. 110585, Feb. 2022, doi: 10.1016/j.oceaneng.2022.110585.

[6] Y. Zhou, Q. Sun, and X. Shi, "Experimental and numerical study on the parametric roll of an offshore research vessel with extended low weather deck," *Ocean Engineering*, vol. 262, p. 111914, Oct. 2022, doi: 10.1016/j.oceaneng.2022.111914.

[7] X. Sun, Y. Ni, C. Liu, Z. Wang, and Y. Yin, "A practical method for stability assessment of a damaged ship," *Ocean Engineering*, vol. 222, p. 108594, Feb. 2021, doi: 10.1016/j.oceaneng.2021.108594.

[8] G. Rosano, E. Begović, G. Boccadamo, and B. Rinauro, "Second Generation Intact Stability Criteria Fallout on Naval Ships Limiting KG Curves," 2020. doi: 10.3233/PMST200047.

[9] N. Petacco, V. Ruggiero, and P. Gualeni, "An Investigation about Stability in Waves of Large Pleasure Yachts," *J Mar Sci Eng*, vol. 11, no. 11, p. 2039, Oct. 2023, doi: 10.3390/jmse11112039.

[10] V. M. ZoBell, M. Gassmann, L. B. Kindberg, S. M. Wiggins, J. A. Hildebrand, and K. E. Frasier, "Retrofit-induced changes in the radiated noise and monopole source levels of container ships," *PLoS One*, vol. 18, no. 3, p. e0282677, Mar. 2023, doi: 10.1371/journal.pone.0282677.

[11] S. Munakata *et al.*, "An investigation into false-negative cases for low-freeboard ships in the vulnerability criteria of dead ship stability," *Ocean Engineering*, vol. 266, p. 113130, Dec. 2022, doi: 10.1016/j.oceaneng.2022.113130.

[12] M. Pricop, "Comparative study of the safety of two tugboats using new harmonized stability rules," *Scientific Bulletin of Naval Academy*, vol. XXV, no. 1, pp. 115–127, Aug. 2022, doi: 10.21279/1454-864X-22-I1-013.

[13] X. Zhang *et al.*, "A numerical investigation on the effect of symmetric and asymmetric flooding on the damage stability of a ship," *J Mar Sci Technol*, vol. 25, no. 4, pp. 1151–1165, Dec. 2020, doi: 10.1007/s00773-020-00706-9.

[14] K. A. Hossain, N. Hasan, T. A. Sohan, and S. M. I. Mahmud, "Effect of Length on the Stability of a Ship," *SSRN Electronic Journal*, 2023, doi: 10.2139/ssrn.4443824.

[15] X. Sun, Y. Ni, C. Liu, Z. Wang, and Y. Yin, "A practical method for stability assessment of a damaged ship," *Ocean Engineering*, vol. 222, p. 108594, Feb. 2021, doi: 10.1016/j.oceaneng.2021.108594.

[16]L.-E. Huynh, C.-R. Chu, and T.-R. Wu, "Hydrodynamic loads of the bridge decks in wave-current combined flows," *Ocean Engineering*, vol. 270, p. 113520, Feb. 2023, doi: 10.1016/j.oceaneng.2022.113520.

[17]T. Pujol *et al.*, "Sensitivity analysis of a particle retention model and application to a pressurised sand bed filter for drip irrigation," *Biosyst Eng*, vol. 230, pp. 51–70, Jun. 2023, doi: 10.1016/j.biosystemseng.2023.04.006.

[18]F. Grinnaert, J.-Y. Billard, and J.-M. Laurens, "KGmax curves associated with second generation intact stability criteria for different types of ships," *Journal of Marine Science and Application*, vol. 15, no. 3, pp. 223–235, Sep. 2016, doi: 10.1007/s11804-016-1369-3.

[19]G. Taimuri, P. Ruponen, and S. Hirdaris, "A novel method for the probabilistic assessment of ship grounding damages and their impact on damage stability," *Structural Safety*, vol. 100, p. 102281, Jan. 2023, doi: 10.1016/j.strusafe.2022.102281.

[20]A. Mentes and H. Akyildiz, "Criticality analysis of probabilistic damage stability of ships with aggregation operators and additive ratio assessment," *Ocean Engineering*, vol. 270, p. 113577, Feb. 2023, doi: 10.1016/j.oceaneng.2022.113577.

[21]K. E. Marlantes, S. (Peter) Kim, and L. A. Hurt, "Implementation of the IMO Second Generation Intact Stability Guidelines," *J Mar Sci Eng*, vol. 10, no. 1, p. 41, Dec. 2021, doi: 10.3390/jmse10010041.

[22]N. Petacco and P. Gualeni, "The influence of ship stability in waves on naval vessel operational profiles," *J Ocean Eng Mar Energy*, vol. 9, no. 4, pp. 681–695, Nov. 2023, doi: 10.1007/s40722-023-00291-0.

[23]W. Mironiuk, "Influence of flooding compartments on the stability safety of the training warship," *Journal of KONBiN*, vol. 42, no. 1, pp. 75–92, Jun. 2017, doi: 10.1515/jok-2017-0019.

[24]J. Zhang, M. C. Ong, and X. Wen, "A Numerical Model for Stability and Dynamic Analyses of a Floating Dock During Operations," *IEEE Journal of Oceanic Engineering*, vol. 49, no. 4, pp. 1160–1182, Oct. 2024, doi: 10.1109/JOE.2024.3436768.

[25]G. Bulian and A. Francescutto, "Level 1 vulnerability criterion for the dead ship condition: A practical methodology for embedding operational limitations," *Ocean Engineering*, vol. 272, p. 113868, Mar. 2023, doi: 10.1016/j.oceaneng.2023.113868.

[26]K. Park, J. Ku, J. Lee, and N. Ku, "Real-time ship stability evaluation program through deterministic method based on second-generation intact stability," *International Journal of Naval Architecture and Ocean Engineering*, vol. 15, p. 100526, 2023, doi: 10.1016/j.ijnaoe.2023.100526.

[27]D. Vassalos, M. P. Mujeeb-Ahmed, D. Paterson, F. Mauro, and F. Conti, "Probabilistic Damage Stability for Passenger Ships—The p-Factor Illusion and Reality," *J Mar Sci Eng*, vol. 10, no. 3, p. 348, Mar. 2022, doi: 10.3390/jmse10030348.